Unimolecular Fragmentation of CH_3NH_2: Towards a Mechanistic Description of HCN Formation

Jana Roithová,[a][‡] Detlef Schröder,*[a] and Helmut Schwarz[a]

Dedicated to Professor Manfred Hesse on the occasion of his 70th birthday

Keywords: Density functional calculations / Dehydrogenation / Mass spectrometry / Methylamine

The mechanism of the consecutive fragmentation of methylamine, CH_3NH_2, is studied by means of neutralization-reionization mass spectrometry (NRMS), labeling experiments, and calculations employing density functional theory. It is shown that under the conditions of NRMS the fragmentations proceed by a radical mechanism that involves four distinct X–H bond cleavages (X = C, N). In the first step, a hydrogen atom is eliminated from the methyl group; next, homolytic cleavage of an N–H bond occurs. The so-formed CH_2NH intermediate then, in competition, releases a hydrogen atom either from the nitrogen or the carbon part, resulting in the formation of the radicals $H_2CN^{\cdot}$ and $HCNH^{\cdot}$, respectively. The reaction sequence is terminated by yet another homolytic bond cleavage to produce HCN. An alternative pathway proceeding by an initial 1,1-elimination of H_2 from the methyl group of CH_3NH_2, followed by a 1,1-elimination of H_2 from the amino function, is also considered, but found to be more energy-demanding.

Introduction

The decomposition of methylamine is linked to some of the essential steps on the way from simple compounds like methane and ammonia to more complex bioorganic molecules.[1] Actually, it was methylamine which was found to be primarily formed upon the action of electric discharges or ultraviolet light on mixtures of methane and ammonia.[2–4] Under these conditions, the reaction proceeds further to yield HCN as a final product. The mechanism of the photofragmentation of CH_3NH_2, i.e. fragmentation on the excited potential-energy surface, has been addressed both experimentally and theoretically because this process is believed to proceed under prebiotic conditions. It has been shown that the mechanism of dehydrogenation depends on the wavelength of the light used in the experiment.[5] At longer wavelengths (184.9 and 222 nm), the expulsion of hydrogen atoms dominates, with the first hydrogen atom being lost by homolytic cleavage of an N–H bond.[6–8] At 147 nm, the 1,2-elimination of molecular hydrogen also becomes important.[9] The interpretation of the experimental results and the fragmentation mechanisms derived from them have been supported by theoretical investigations.[10,11]

An early study of the thermal decomposition of CH_3NH_2 suggested that the unimolecular fragmentation leads to HCN + 2 H_2, and that the initial reaction step is associated with a large activation energy (ca. 2.5 eV).[12] Later, the reaction was also investigated in a hot-filament chemical-vapor deposition reactor.[13] As to the possible mechanism, successive hydrogen-atom abstractions to produce HCN have been suggested, with formimine, CH_2NH, being a central intermediate. However, the proposed mechanisms are by and large rather speculative since no intermediates were observed. The theoretical work related to the electronic ground state of CH_3NH_2[14] also comprises an RRKM study of the dehydrogenation of CH_3NH_2.[15] According to these investigations, the energetically most favored pathway corresponds to a 1,1-elimination of H_2 from the methyl group, with an activation energy of 3.46 eV; the alternative routes of a 1,2- and a 1,1-elimination (the latter involving the NH_2 group) are associated with calculated barriers more than 1 eV higher in energy, i.e., 4.56 eV and 4.91 eV, respectively.

In this paper the consecutive fragmentations of CH_3NH_2 are studied by means of neutralization-reionization mass spectrometry and complemented by calculations using density functional theory.

[a] Institut für Chemie der Technischen Universität Berlin, 10623 Berlin, Germany
Fax: +49-30-314-21102
E-mail: Detlef.Schroeder@TU-Berlin.de
[‡] Present address: J. Heyrovský Institute of Physical Chemistry, Academy of Sciences of the Czech Republic, 18223 Praha 8, Czech Republic

  DOI: 10.1002/ejoc.200500029

Results and Discussion

The present study on the mechanism of the gas-phase reaction $CH_3NH_2 \rightarrow HCN + 2\ H_2$ uses the methodology of neutralization-reionization (NR) mass spectrometry.[16–21] In these experiments, neutral molecules are generated from a precursor ion in a collision event taking place at a translational energy of 8 keV. The connectivity and the unimolecular fragmentations of the precursor ions can, and have to, be probed in separate experiments. Thus, the precursor ions − cations or anions − are generated and mass-selected. In the next step, the ions are neutralized in a collision with an appropriate gas and all remaining charged species are deflected. In the third step, the neutral parent molecule and its eventual fragments are reionized in a time-delayed further collision in order to permit mass spectrometric detection. In an ideal case which assumes that (i) the precursor ion itself does not fragment upon collision, (ii) the ionization cross-sections of all neutral particles are the same, and (iii) the reionized particles do not undergo further fragmentations, the NR mass spectrum would show the unimolecular fragmentations of the neutral molecule in the gas phase. However, the ionization cross-sections differ and fragmentations of the reionized particles are often quite extensive. Therefore, several approaches have been developed to extract the desired information on the neutrals' reactivity.[16,17] Here, the following methods are used: (i) neutralization followed by collisional activation and reionization (NCR), (ii) variation of lifetimes of the transient neutral molecules, and (iii) the neutral and ion decomposition difference (NIDD) scheme.[22]

The neutralization experiments involve the cation radical $CH_3NH_2^{+\cdot}$; the use of the corresponding anion radical $CH_3NH_2^{-\cdot}$ is impossible because the anion undergoes rapid loss of a hydrogen atom to form CH_3NH^-. The internal energy deposition in CH_3NH_2 upon vertical reduction of $CH_3NH_2^{+\cdot}$ has been studied by Nguyen and Tureček.[23] They concluded that collisional neutralization of $CH_3NH_2^{+\cdot}$ formed by electron ionization leads to the electronic ground state of CH_3NH_2 and is associated with a deposition of about 1 eV of rovibrational excitation. As electron transfer in keV collisions can be considered to occur as a vertical process, the deposition of internal energy can be roughly estimated from the differences between vertical and adiabatic recombination (or ionization) energies ($\Delta E_{v/a}$). This simplified approach leads to a value of $\Delta E_{v/a}$ of 0.31 eV as a lower estimate for the internal energy deposited upon vertical neutralization of $CH_3NH_2^{+\cdot}$. The discrepancy between this value and that derived from experimental data[23] can most likely be attributed to a mismatch between the actual experiment and the idealized model assumption that the reaction energy needed or released during the charge transfer is taken from the kinetic energy of projectiles or transferred to the kinetic energy of products, while neither kinetic nor reaction energy contributes to the internal energies of products. In a real experiment, however, a conversion between the kinetic or reaction energy and the internal energy certainly takes place. Moreover, and besides other factors, the energy balance of the charge-transfer process, and thus the ionization energy (*IE*) of the collision gas, also plays a role in that the larger endothermicity or exothermicity leads to a larger deposition of internal energy.[24] To estimate this effect, the $^+NR^+$[25] spectra of $CH_3NH_2^{+\cdot}$ were measured with xenon and propene as neutralization gases (Table 1). As expected, a smaller endothermicity for the charge transfer between $CH_3NH_2^{+\cdot}$ and propene leads to a slightly enhanced intensity of the recovery signal (37%) compared to charge exchange between $CH_3NH_2^{+\cdot}$ and xenon (31%). In the work of Nguyen and Tureček,[23] neutralization gases with ionization energies even closer to that of methylamine were used; nevertheless, the recovery signal in the published spectrum[23] is of lower relative abundance, concomitant with more pronounced fragmentations than is found in the present work. Most probably, the different experimental settings account for these moderate discrepancies. Hence, the estimate of 1 eV of the internal energy deposition[23] appears somewhat higher than is expected for the present experiments.

Table 1. $^+NR^+$ spectra[a] of mass-selected $CH_3NH_2^{+\cdot}$ (m/z = 31) generated by EI of methylamine as a function of the ionization energy of the different collision gases used for neutralization.[b]

Neutralization gas	Xe	Propene
IE(collision gas)	12.1 eV	9.7 eV
Δ*E*(charge transfer)	3.2 eV	0.8 eV
m/*z*		
31	31	37
30	54	57
29	3	1
28	8	4
27	3	1
26	1	0.2

[a] Intensities correspond to peak heights; the sum of intensities was set to 100. [b] Oxygen was used as reionization gas in both experiments.

In the following, experiments with the labeled precursor CD_3NH_2 are described because this compound allows some differentiation between the hydrogen atoms at carbon and nitrogen. The metastable ion (MI) spectrum of $CD_3NH_2^{+\cdot}$ shows a specific loss of a deuterium atom from the methyl group (Table 2). Upon collisional activation (CA), a number of consecutive dissociations as well as direct bond cleavages are observed, while elimination of $D^{\cdot}$ still predominates. The fragments and also their relative intensities observed in the neutralization-reionization spectrum (Figure 1a) by and large resemble those formed upon CA, thus indicating that the fragmentations preferentially occur in the charged state and, as expected, the neutral amine is quite stable. The comparison of the two $^+NR^+$ spectra with different flight times of the neutral species can reveal possible fragmentations occurring at the neutral stage.[16,17] The experimental approach uses the advantage of three collision cells mounted in one field-free region of the Berlin four-sector instrument. In the long-distance $^+NR^+$ experiment, neutralization of the ionic precursor occurs in the first collision cell, whereas the second collision cell is used for that purpose in the short-distance $^+NR^+$. In both experiments,

reionization takes place in the third collision cell. Thus, the time window in which the reionized species undergo fragmentation prior to detection remains the same, whereas the flight time of the neutral transient is greater in long-distance $^{+}NR^{+}$ than in short-distance $^{+}NR^{+}$. For example, the flight time of neutral CD_3NH_2 amounts to 0.5 μs for short-distance $^{+}NR^{+}$ compared to 4.2 μs in long-distance $^{+}NR^{+}$. When the overall intensities of both spectra are normalized, subtraction of the short-distance $^{+}NR^{+}$ spectrum from the long-distance $^{+}NR^{+}$ one leads to a difference spectrum in which positive signals indicate processes preferentially occurring at the neutral stage, whereas negative signals indicate predominant fragmentations of reionized cations. The sensitivity of this method is satisfactory if the neutral species show significant fragmentations; otherwise, the results can be taken only as a qualitative guide. Moreover, two potential drawbacks have to be considered. Firstly, the results are informative only when the fragmentation of the metastable precursor ion, which precedes neutralization, is negligible. If this does not hold true, then the unimolecular fragmentations appear as negative signals. Secondly, the lighter neutral particles are more scattered than the heavier ones, which leads to their discrimination in the long-distance $^{+}NR^{+}$; thus, qualitatively correct results are expected only in regions of similar *m*/*z* ratios, and therefore only the mass region of *m*/*z* = 26–34 is considered relevant here. The difference between short- and long-distance $^{+}NR^{+}$ spectra (Figure 1b) shows that the dominant process in *neutral* CD_3NH_2 corresponds to the loss of a D˙ atom (*m*/*z* = 32), i.e., homolytic cleavage of a C–D bond prevails over scission of an N–H bond.

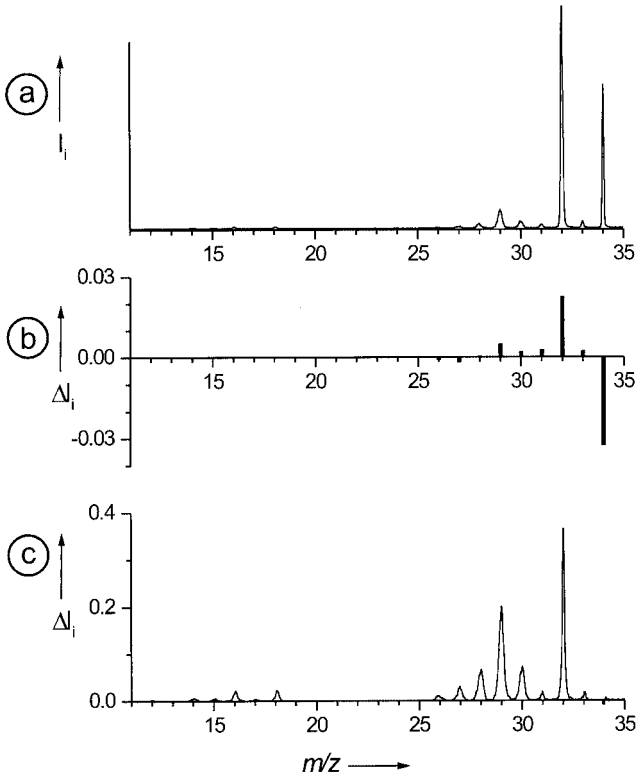

Figure 1. a) Long-distance $^{+}NR^{+}$ spectrum, b) difference between long- and short-distance $^{+}NR^{+}$ spectra (ΣI_i = 1 for each), and c) difference between long-distance $^{+}NR^{+}$ and $^{+}NCR^{+}$ with *T*(He) = 80% of mass-selected $CD_3NH_2^{+\cdot}$ generated by EI of CD_3NH_2. In the latter case, for each individual spectrum the intensities are normalized to the intensity of the survivor ion $CD_3NH_2^{+\cdot}$ (*m*/*z* = 34), which is set to 1.

Table 2. MI and CA spectra of mass-selected cations generated by EI of CD_3NH_2.

Precursor ions[a,b] *m*/*z*	$CD_3NH_2^{+\cdot}$ 34		$CD_2NH_2^{+}$ 32		$CD_2NH^{+\cdot}$ 31		$CDNH^{+}$ 29	
Fragment ions (*m*/*z*)	MI	CA	MI	CA	MI	CA	MI	CA
33		4.3						
32	0.2	100						
31		3.5		1.3				
30		24		13	0.1	56		
29		76	0.2	100	0.03	100		
28		19		26		28	0.1	100
27		7.3		12		12		68
26		1.9		2.6		4.1		28
18		1.7		0.1		0.1		
17				0.2		0.4		0.4
16		1.5		2.2		1.1		0.6
15				0.4		0.7		1.8
14				0.6		1.0		2.8
13						0.1		0.3
12				0.2		0.2		1.0

[a] Intensities correspond to integrated peak areas; base peak normalized to 100. In the MI spectra, the base peak corresponds to the parent ion. [b] Predominant isomer.

Alternatively, the fragmentation of the neutral molecule can be probed by inserting a collisional activation step into the NR sequence ($^{+}NCR^{+}$).[26] This kind of experiment uses three collision cells located in one field-free region in the following manner: Neutralization of the mass-selected ionic precursor is achieved in the first cell, reionization in the third, and the central cell is used for collisional activation of the neutral transient with helium. The dependence of fragment-ion intensities on the helium pressure in the collision cell, which is expressed by means of the transmission (*T*), is shown in Figure 2. The intensity of the recovery ion $CD_3NH_2^{+\cdot}$ is normalized to 1, and for all other ions the abundances increase with decreasing transmittance. The slopes of the individual curves indicate the increase of the respective fragmentations upon CA of the neutral species. In Figure 1c, the difference between the spectra with 80% and 100% transmissions is evaluated. Thus, the collisional activation of neutral CD_3NH_2 leads again to a more pronounced elimination of D˙. In the interpretation of the $^{+}NCR^{+}$ spectrum, it is necessary to keep in mind that the increase of a particular neutral fragment also enhances the specific fragmentations of the corresponding reionized species. Thus, the collision-induced formation of $CD_2NH_2^{\cdot}$ leads not only to a more abundant signal of $CD_2NH_2^{+}$, but also the abundances of the ions $CDNH_2^{+}/CD_2N^{+}$ (both *m*/*z* = 30), $CDNH^{+}$ (*m*/*z* = 29), and DCN^{+} (*m*/*z* = 28) are enhanced due to the subsequent fragmentations of the cation $CD_2NH_2^{+}$ formed upon reionization (see below). From Figure 1c, we conclude that the fragmentation of CD_3NH_2 starts with the loss of a D˙ atom.

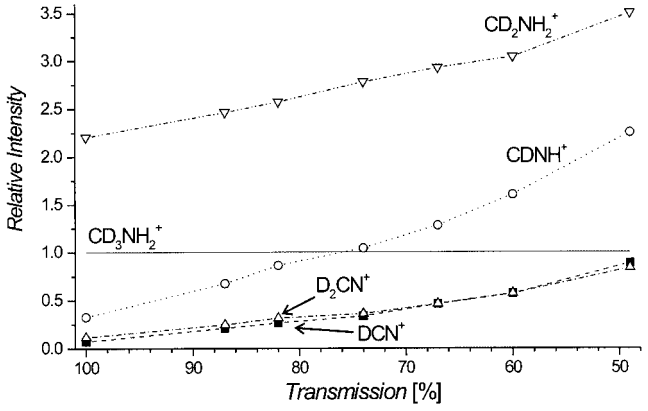

Figure 2. Intensities of major fragment-ion signals in the $^+NCR^+$ spectrum of $CD_3NH_2^{+\cdot}$ as a function of helium pressure (expressed by means of transmission). The intensities are normalized to the intensity of the survivor ion $CD_3NH_2^{+\cdot}$, which is set to 1.

Next, let us compare the experimental results with the computational findings. As mentioned in the Introduction, the unimolecular fragmentation of CH_3NH_2 has been the subject of several theoretical studies. To compare all results at a common level, and also to substantially augment the existing data, B3LYP calculations were performed. The energetically most favored pathway for the decomposition of CH_3NH_2 corresponds to dehydrogenation by a 1,1-elimination from the methyl group with an associated transition structure lying 3.28 eV above CH_3NH_2 (Scheme 1). Other pathways for H_2 eliminations proceed via higher barriers, as already discussed in ref.[15] For example, 1,2-elimination of H_2 is associated with a barrier of 4.39 eV. The 1,1-elimination of H_2 from the NH_2 group is coupled with a hydrogen rearrangement from the carbon to the nitrogen atom, thus leading again to formimine. This mechanism is associated with a transition structure lying 4.70 eV above methylamine. An analogous behavior has also been observed for the unimolecular fragmentation of methyl azide, CH_3N_3. Here, the elimination of N_2 is associated with a hydrogen rearrangement leading directly to CH_2NH as the product.[27] The 1,1-elimination to afford CH_3N on the singlet surface, as proposed in ref.[15], is considered improbable, because CH_3N is a biradical with a triplet ground state;[28] thus, the process must be connected with a spin change[29] or it would lead to a higher excited state. In addition, it should be noted that all transition structures for concerted H_2 eliminations are very tight and thus entropically disfavored. In the following, only the energetically favored 1,1-elimination from the methyl group is considered. Accordingly, dehydrogenation of CD_3NH_2 should lead to $CDNH_2$. However, the signal at m/z = 30 is quite small in the $^+NR^+$ spectrum (Figure 1a); moreover, isobaric $CD_2N^{+\cdot}$ also contributes to this signal. In the $^+NR^+$ spectrum of nonlabeled $CH_3NH_2^{+\cdot}$, the corresponding fragment ion $CHNH_2^{+\cdot}$ also gives rise to only a small signal and suffers from superposition with the isomeric ion $CH_2NH^{+\cdot}$. For other labeled precursors, such as CH_3ND_2, similar superpositions are expected. Thus, unambiguous experimental information on this particular fragmentation channel is difficult to obtain. Nevertheless, it can be concluded that under $^+NR^+$ conditions the elimination of a hydrogen radical clearly dominates over that of molecular hydrogen. While the energy required for the direct C–H bond cleavage is 0.54 eV higher than the barrier associated with H_2 elimination (Scheme 1), the direct C–H bond cleavage is certainly associated with a much higher density of states than the tight transition structure associated with H_2 elimination. Consequently, a kinetic preference of the single bond cleavage pathway can be anticipated under NR conditions.

Next, the fragmentation of the aminomethyl radical is addressed, which is also studied for the labeled species $CD_2NH_2^{\cdot}$. The neutral radical is generated from the corresponding fragment ion $CD_2NH_2^+$ formed by EI of CD_3NH_2. The CA spectrum of $CD_2NH_2^+$ shows that the connectivity of the cation is conserved (Table 2). Neutralization of $CD_2NH_2^+$ is associated with internal excitation of about $\Delta E_{v/a}$ = 0.39 eV. Like upon CA, the most abundant fragmentation process in the $^+NR^+$ spectrum of $CD_2NH_2^+$ (Figure 3a) corresponds to the loss of HD (m/z = 29). The major difference between the CA and $^+NR^+$ spectra is the more pronounced $H^{\cdot}$ elimination in $^+NR^+$, which represents a negligible channel in the CA spectrum of $CD_2NH_2^+$. A comparison of the long-distance and short-distance $^+NR^+$ spectra of $CD_2NH_2^+$ (Figure 3b) also suggests preferential loss of $H^{\cdot}$ from the neutral radical. Interestingly, the $^+NCR^+$ spectrum (Figure 3c) shows that the intensity of the signal corresponding to $H^{\cdot}$ loss decreases even though this process is suggested as the dominant initial fragmentation step of the neutral radical. This can be explained by the involvement of either competing channels or subsequent fragmentations. The other fragmentations in the $^+NCR^+$ spectrum are similar to those found for CD_3NH_2, i.e. the formation of $DCNH^{\cdot}$, DCN, and $CN^{\cdot}$. It is worth mentioning that the signal corresponding to m/z = 30, i.e.

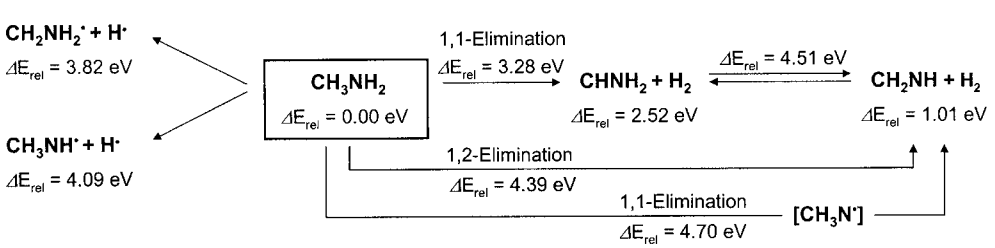

Scheme 1. B3LYP-calculated pathways for possible $H^{\cdot}$ and H_2 eliminations from CH_3NH_2. Energies are given in eV at 0 K relative to CH_3NH_2 (E_{tot} = –95.8958363 Hartree, ZPVE = 0.063811 Hartree). See text for details.

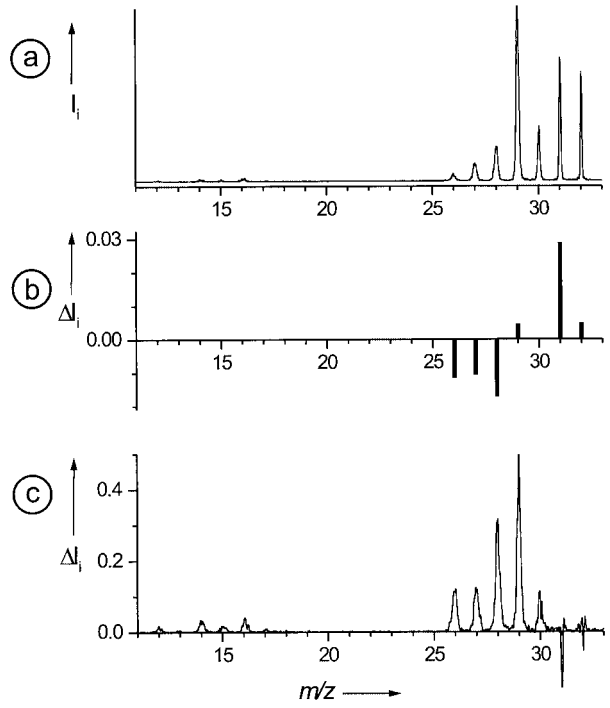

Figure 3. a) Long-distance $^{+}NR^{+}$ spectrum, b) difference between long- and short-distance $^{+}NR^{+}$ spectra (ΣI_i = 1 for each), and c) difference between long-distance $^{+}NR^{+}$ and $^{+}NCR^{+}$ with T(He) = 80% of mass-selected $CD_2NH_2^{+}$ generated by EI of CD_3NH_2. In the latter case, for each individual spectrum the intensities are normalized to the intensity of the survivor ion $CD_2NH_2^{+}$ (m/z = 32), which is set to 1.

$CDNH_2$ or CD_2N, is less intense than in the $^{+}NCR^{+}$ spectrum of $CD_3NH_2^{+\cdot}$ (Figure 1c). This finding may indicate a different mechanism for the formation of $CDNH_2/CD_2N$ from CD_3NH_2, specifically, a 1,1-elimination of D_2 from CD_3NH_2, as mentioned above.

Further insight into the fragmentation mechanism of $CH_2NH_2^{\cdot}$ can again be obtained from a comparison of the experimental data with the potential-energy surface (PES) of $[CH_4N]^{\cdot}$ (Scheme 2). The radical $CH_2NH_2^{\cdot}$ is the most stable isomer. The least energy-demanding dissociation pathway corresponds to the loss of a hydrogen atom from the NH_2 group with an associated barrier of 1.74 eV, only slightly above the reaction endothermicity (1.69 eV). The alternative hydrogen elimination from the methylene group requires 3.19 eV. The barrier for isomerization of $CH_2NH_2^{\cdot}$ to $CH_3NH^{\cdot}$ requires only 1.89 eV, such that partial isomerization and thus hydrogen scrambling in neutral $[CH_4N]^{\cdot}$ may be expected. Nevertheless, the preferred fragmentation of the $CH_3NH^{\cdot}$ isomer also leads to CH_2NH; an alternative elimination of a hydrogen atom from the NH group would lead to the biradical CH_3N in its triplet ground state,[28] which lies 2.14 eV higher in energy than CH_2NH.

The further elimination of a hydrogen atom from formimine, CH_2NH, is associated with large endothermicities (Scheme 2): cleavage of the N–H bond requires an additional energy of 3.61 eV and that of the C–H bond demands 3.97 eV. The concerted elimination of molecular hydrogen from $CH_2NH_2^{\cdot}$ and $CH_3NH^{\cdot}$, respectively, is also associated with large barriers, not to mention the tightness

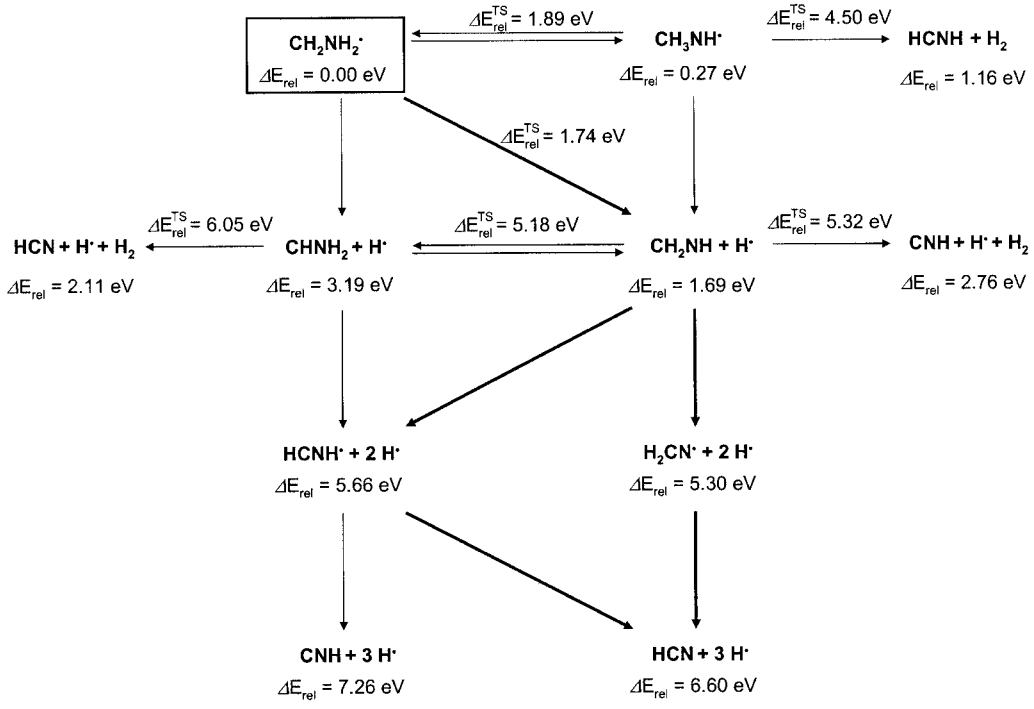

Scheme 2. Potential-energy surface of $[CNH_4]^{\cdot}$ calculated at the B3LYP level of theory. Energies are given in eV at 0 K, relative to $CH_2NH_2^{\cdot}$ (E_{tot} = –95.23928 Hartree, ZPVE = 0.049897 Hartree). See text for details.

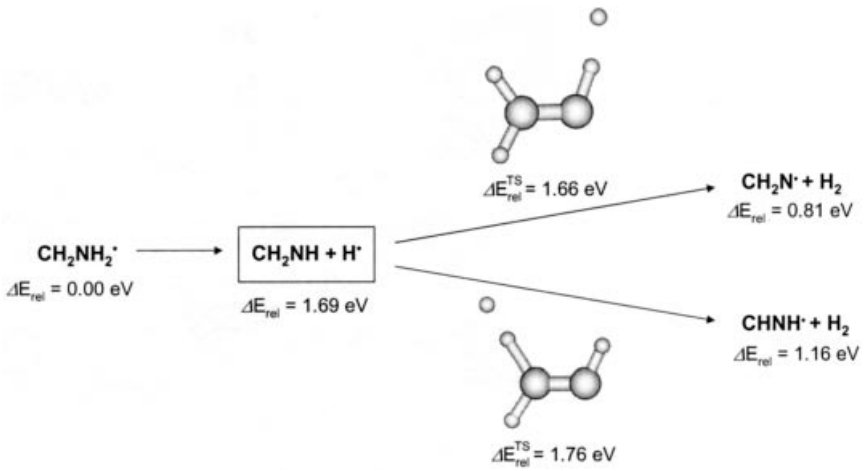

Scheme 3. Sketch of the proposed abstraction of a hydrogen atom from formimine CH_2NH by a hydrogen radical, leading to the formation of molecular hydrogen.

of the transition structures. The barrier for a 1,1-elimination of H_2 from $CH_3NH^{\cdot}$ amounts to 4.23 eV. The barrier for a 1,2-elimination of H_2 from $CH_2NH_2^{\cdot}$ could not be located, but it can be expected that the situation is similar to that found for H_2 elimination from the cation $CH_2NH_2^{+\cdot}$.[30] The 1,2-elimination pathway is connected with an intramolecular hydrogen rearrangement which involves a bifurcation point.[31] Thus, the barrier presumably lies in the energy range from 1.89 to 4.50 eV.

Another, less energy-demanding mechanism for a "stepwise" elimination of H_2 is proposed in Scheme 3: in a putative pair of $CH_2NH + H^{\cdot}$ formed initially, the hydrogen radical assists the elimination of the second hydrogen atom in that molecular hydrogen evolves. The barriers associated with such an elimination mechanism of dihydrogen are in the range of the energy needed for the initial N–H bond cleavage (ΔE_{rel} = 1.69 eV), because the elimination of the second hydrogen atom from both nitrogen and carbon is subject to very small energy barriers. For the elimination of the second hydrogen atom from the NH group, this barrier lies even below the putative pair $CH_2NH + H^{\cdot}$ when zero-point vibrational energy is included. Such a scenario, i.e. a radical-assisted hydrogen-atom abstraction leading to a closed-shell molecule, can, of course, become particularly important under high-pressure conditions.

With the complementary information provided by theory, let us now return to the experimental results. The signal at m/z = 31 in the $^+NR^+$ spectrum of $CD_2NH_2^+$ is representative for N–H cleavage. A decrease of the intensity of m/z = 31 upon collisional activation in the $^+NCR^+$ experiment can be ascribed to subsequent fragmentation of CD_2NH itself, leading to the loss of another hydrogen atom, or due to the competition between elimination of $H^{\cdot}$ and that of molecular hydrogen from $CD_2NH_2^{\cdot}$. In the present context, a "stepwise" H_2 (HD) elimination can be excluded because it requires the formation of a putative $CD_2NH{\cdot}H^{\cdot}$ complex, which is less likely to survive long enough at higher internal energies, i.e. upon collisional activation. Therefore, we are left with the alternative of a concerted elimination mechanism of molecular hydrogen. However, these fragmentation pathways proceed via barriers similar to the energy required for two successive hydrogen-atom eliminations and are therefore disfavored on the basis of density of states, as discussed above for the H_2 elimination from CH_3NH_2. Thus, the decrease of the $CD_2NH^{+\cdot}$ signal most probably does not originate from the competition between the two channels, but is rather due to a subsequent elimination of a second hydrogen atom, either $D^{\cdot}$ or $H^{\cdot}$.

The signal at m/z = 30 in Figure 3a can originate either from the elimination of a $D^{\cdot}$ atom or from sequential removal of two $H^{\cdot}$ atoms. Elimination of a deuterium atom would lead to $CDNH_2$, which is less stable than CD_2NH. Therefore, a similarly efficient subsequent fragmentation as found for CD_2NH would be expected, leading to a negative signal in the $^+NCR^+$ spectrum. In contrast, an increase of m/z = 30 is observed; most probably, the major contribution to m/z = 30 can thus be ascribed to the consecutive fragmentation $CD_2NH_2^{\cdot} \rightarrow CD_2NH \rightarrow CD_2N^{\cdot}$. The formation of $CDNH^{\cdot}$ (m/z = 29) can be also explained by consecutive reactions involving the eliminations of hydrogen atoms: $CD_2NH_2^{\cdot} \rightarrow CD_2NH \rightarrow CDNH^{\cdot}$. However, the competition between elimination of a second hydrogen atom from either nitrogen or carbon is expected to favor N–H bond cleavage because the cleavage of a C–D bond is 0.33 eV more energy-demanding (neglecting isotope effects). The fact that the signals due to $CDNH^{\cdot}$ are larger than those of $CD_2N^{\cdot}$ in the $^+NCR^+$ spectrum as well as in the difference between long- and short-distance $^+NR^+$ spectra is attributed to the reionization of $CD_2N^{\cdot}$, which primarily leads to DCN^+ rather than CD_2N^+ (see below).

The conclusions drawn so far were once more probed in separate experiments concerning the subsequent fragmentation of CD_2NH. The corresponding precursor ion $CD_2NH^{+\cdot}$ was generated by dissociative EI of CD_3NH_2. The CA spectrum of $CD_2NH^{+\cdot}$ (Table 2) shows that the major fraction of the ions with m/z = 31 has indeed the connectivity of the desired $CD_2NH^{+\cdot}$ isomer; nevertheless,

the isomer $CDNHD^{+\cdot}$ can be also populated, as indicated by the fragment ion $NHD^{+\cdot}$ (m/z = 17). Neutralization of $CD_2NH^{+\cdot}$ is associated with a considerable Franck–Condon excitation energy ($\Delta E_{v/a}$ = 0.82 eV), which is mostly due to a large change of the C–N–H angle (from 151° to 111°). The $^{+}NR^{+}$ spectrum (Figure 4a) shows an approximate 1:2 ratio of $H^{\cdot}$ and $D^{\cdot}$ atom losses. The comparison of long- and short-distance $^{+}NR^{+}$ (Figure 4b) suggests that both eliminations occur at the neutral stage. The dominant peak in the $^{+}NCR^{+}$ spectrum of $CD_2NH^{+\cdot}$ (Figure 4c) corresponds to the formation of $DCN^{+\cdot}$ (m/z = 28). In part, this signal comes from dissociative reionization of $CD_2N^{\cdot}$ (see below); nevertheless, the increased relative intensity in comparison to Figure 3c suggests that both $CDNH^{\cdot}$ and $CD_2N^{\cdot}$ contribute to the formation of m/z = 28 via subsequent fragmentation steps.

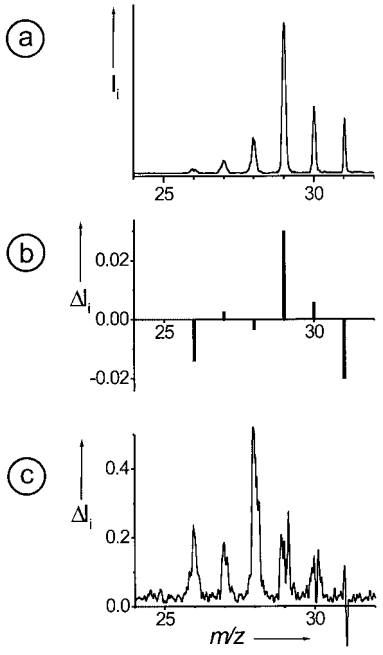

Figure 4. a) Long-distance $^{+}NR^{+}$ spectrum, b) difference between long- and short-distance $^{+}NR^{+}$ spectra (ΣI_i = 1 for each), and c) difference between long-distance $^{+}NR^{+}$ and $^{+}NCR^{+}$ with T(He) = 80% of mass-selected $CD_2NH^{+\cdot}$ generated by EI of CD_3NH_2. In the latter case, for each individual spectrum the intensities are normalized to the intensity of the survivor ion $CD_2NH^{+\cdot}$ (m/z = 31), which is set to 1.

The radical $CD_2N^{\cdot}$ can be generated easily from the corresponding anion CD_2N^{-} formed upon negative-ion chemical ionization (CI) of CD_3NH_2 without additional reagent gas.[32] Accordingly, the method of neutral and ion decomposition difference ($^{-}NIDD^{+}$)[17] can be used. This method consists of a comparison of $^{-}NR^{+}$ (Figure 5a) and charge-reversal ($^{-}CR^{+}$) spectra in the same manner as described for the long- and short-distance $^{+}NR^{+}$. Thus, positive signals are due to fragmentations occurring at the neutral stage, and negative signals originate from preferential decompositions of ionic species. The $^{-}NIDD^{+}$ spectrum of $CD_2N^{\cdot}$ (Figure 5b) shows positive signals for the recovery ion CD_2N^{+} and for CN^{+}, whereas DCN^{+} appears as a negative signal. The explanation for this behavior rests on the stability of the cationic species formed upon reionization. A minimum, which would correspond to the singlet cation CH_2N^{+}, could not be located in the calculations.[33] Instead, a stationary point with a planar geometry similar to that of neutral $CH_2N^{\cdot}$ ($\Delta E_{v/a}$ = 0.09 eV) was found to bear an imaginary frequency of i346 cm^{-1}, which is associated with the wagging vibration of the hydrogen atoms, i.e. an antisymmetric vibration in the plane of the radical. This singlet state of CH_2N^{+} lies 2.91 eV above the more stable isomer $HCNH^{+}$. While the triplet state of CH_2N^{+} represents a genuine minimum, it is even higher in energy (4.82 eV above the singlet $HCNH^{+}$); neutralization to the triplet state is associated with $\Delta E_{v/a}$ = 0.36 eV. The formation of CH_2N^{+} by direct charge inversion of the anion CH_2N^{-} is associated with $\Delta E_{v/a}$ = 0.16 eV for the singlet and $\Delta E_{v/a}$ = 0.44 eV for the triplet state. Thus, it can be expected that the recovery signal upon the reionization of $CD_2N^{\cdot}$ or charge reversal of CD_2N^{-} actually represents $DCND^{+}$, which is formed by an easy, presumably barrier-free rearrangement in the singlet cation state.[33,34] The negative signal for DCN^{+} in the $^{-}NIDD^{+}$ spectrum is attributed to a facile loss of a deuterium atom upon formation of the cationic species CD_2N^{+}. This fragmentation of the neutral transient is reflected in the $^{-}NCR^{+}$ spectrum (Figure 5c). As expected, collisional activation leads mainly to the formation of DCN.

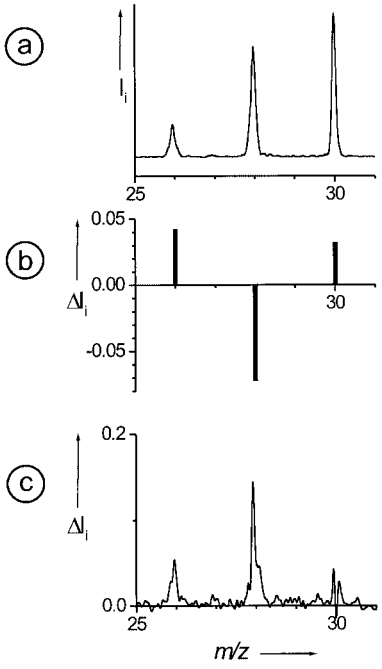

Figure 5. a) $^{-}NR^{+}$ spectrum, b) difference between $^{-}NR^{+}$ and $^{-}CR^{+}$ spectra with ΣI_i = 1 for each ($^{-}NIDD^{+}$ spectrum), and c) difference between the $^{-}NR^{+}$ and $^{-}NCR^{+}$ with T(He) = 80% (ΣI_i = 1 for each) of mass-selected CD_2N^{-} (m/z = 30) generated by negative CI of CD_3NH_2 without additional reagent gas.

The radical $DCNH^{\cdot}$ is generated from the corresponding cation with $\Delta E_{v/a}$ = 1.92 eV. The large internal excitation of the neutral molecule follows from the quite different geometries. For example, the $DCNH^{+}$ cation has a linear geome-

try, whereas the neutral counterpart shows *anti*- or *syn*-periplanar arrangements of the hydrogen and deuterium atoms relative to the C–N backbone. The major signal in the $^+NR^+$ spectrum (Figure 6a) corresponds to the elimination of H$^\cdot$ atom to yield DCN, as expected. A comparison of the long- and short-distance $^+NR^+$ spectra (Figure 6b) reveals the loss of H$^\cdot$ to occur at the neutral stage.

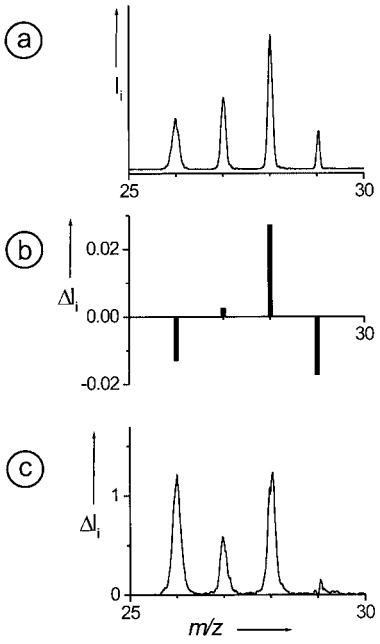

Figure 6. a) Long-distance $^+NR^+$ spectrum, b) difference between long- and short-distance $^+NR^+$ spectra (ΣI_i = 1 for each), and c) difference between the long $^+NR^+$ and $^+NCR^+$ with T(He) = 80% of mass-selected $CDNH^+$ generated by EI of CD_3NH_2. In the latter case, for each individual spectrum the intensities are normalized to the intensity of the survivor ion $CDNH^+$ (m/z = 29), which is set to 1.

Finally, the fragmentation of the aminocarbene,[35] $CHNH_2$, is addressed because it has been proposed[15] as an intermediate in the thermochemically favored fragmentation of methylamine. The perdeuterated precursor $CDND_2^{+\cdot}$ was generated from labeled diethyl 2-aminomalonate $D_2NCD(COOC_2H_5)_2$ by dissociative EI. Neutralization of the cation is associated with $\Delta E_{v/a}$ = 0.60 eV. As expected, the $^+NR^+$ spectrum (Figure 7a) shows consecutive D-atom eliminations; small peaks at odd masses originate from isobaric impurities in the precursor ion. A comparison of the long- and short-distance $^+NR^+$ spectra leads to an interesting result: the dominant change between the two spectra corresponds to the increased abundance of the recovery ion, which suggests that, at longer flight times, a more stable neutral molecule must have been sampled. Most likely, the $CDND_2$ isomer rearranges to formimine, CD_2ND. The subsequent fragmentations are then analogous to those of CD_2NH (see above). A closer look at the $^+NCR^+$ spectrum (Figure 7c) indicates that the elimination of a single D$^\cdot$ atom slightly prevails over elimination of two deuterium atoms. In comparison, the $^+NCR^+$ spectrum of CD_2NH (Figure 4c) shows a larger $DCN^{+\cdot}$ signal than the sum of CD_2N^+ and $CDNH^+$ signals. This discrepancy is most probably due to a contribution of the nonrearranged $CDND_2$ isomer, which dissociates to CDND$^\cdot$ (m/z = 30) and therefore shifts the ratio of $CD_2N^\cdot$ (mostly appearing as $DCN^{+\cdot}$ upon reionization) vs. CDND$^\cdot$ in favor of the second.

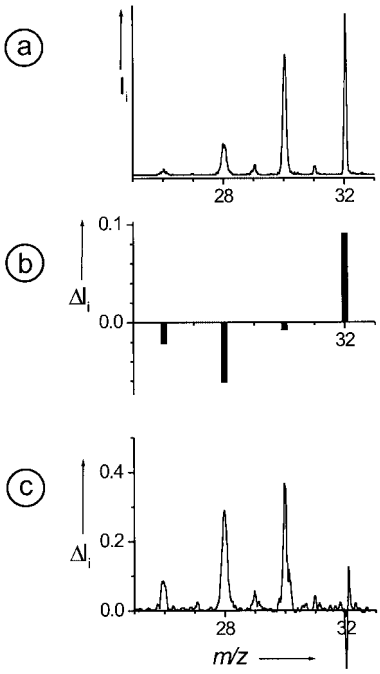

Figure 7. a) Long-distance $^+NR^+$ spectrum, b) difference between long- and short-distance $^+NR^+$ spectra (ΣI_i = 1 for each), and c) difference between long-distance $^+NR^+$ and $^+NCR^+$ with T(He) = 80% of mass-selected $CDND_2^+$ generated by EI of $D_2NCD(COOC_2H_5)_2$. In the latter case, for each individual spectrum the intensities are normalized to the intensity of the survival ion $CDND_2^+$ (m/z = 32), which is set to 1.

Conclusions

The unimolecular fragmentation of methylamine to produce HCN has been probed by a combination of various types of neutralization-reionization (NR) mass spectrometric experiments, complemented with computational studies using density functional theory. In summary, the most probable mechanism for the formation of HCN from methylamine under the conditions of NR starts with a homolytic cleavage of a C–H bond of CH_3NH_2. The so-formed $CH_2NH_2^\cdot$ radical then releases a hydrogen atom from the amine group to yield formimine, CH_2NH. This intermediate subsequently loses, in competition, a hydrogen atom from either the nitrogen or the carbon part. The resulting intermediate radicals, $CH_2N^\cdot$ and CHNH$^\cdot$, respectively, both undergo elimination of atomic hydrogen to finally yield HCN. The alternative 1,1-elimination of H_2 from methylamine leads to a $CHNH_2$ transient which can either consecutively lose hydrogen atoms from the amino group or rearrange to the more stable isomer CH_2NH, which then decomposes as mentioned above.

Experimental Section

The experiments were performed with a modified VG ZAB/HF/AMD four-sector mass spectrometer of *BEBE* configuration (*B* stands for magnetic and *E* for electric sector), which has been described in detail previously.[36] The precursor cations were generated by 70 eV electron ionization and the anions by chemical ionization (CI) without an additional reagent gas (self-CI). The ions formed in the ion source were accelerated to a kinetic energy of 8 keV, mass-selected by means of *B*(1)/*E*(1), and characterized by their metastable ion (MI) and collisional-activation (CA) spectra. To this end, the unimolecular fragmentations of the ions, and their fragmentations upon collision with helium (80% transmission, *T*) in the field-free region preceding the second magnet (3rd FFR), were recorded by scanning *B*(2). The fragmentations of the neutrals were probed by a series of experiments using the three differentially pumped collision cells located in the third FFR of the Berlin sector instrument, which is also equipped with two ion deflectors placed behind the first and the second collision cell in the third FFR. The short-distance neutralization-reionization (NR) and charge-reversal (CR) spectra were obtained by using the second and third cells only. For NR experiments, both cells were filled (80% *T*) with appropriate gases ($^{-}NR^{+}$: O_2 and O_2, respectively; $^{+}NR^{+}$: Xe and O_2, respectively)[25] and the deflector was switched on. For $^{-}CR^{+}$ experiments, only the latter cell was filled with O_2 (80% *T*) while the deflector electrode was grounded. The long-distance NR spectra were obtained in the same manner using the first and the third cell under identical conditions as in the short-distance NR. Neutralization collisional-activation reionization ($^{+}NCR^{+}$ and $^{-}NCR^{+}$) spectra were obtained using all three cells filled with Xe/He/O_2 (80% *T*) and O_2/He/O_2 (80% *T*), respectively. In the $^{+}NCR^{+}$ experiment, the pressure of He was varied (see text). All spectra were accumulated with the AMD-Intectra data systems; usually 10–50 scans were averaged to improve the signal-to-noise ratio. The data given here were derived from three to six independent measurements with the final experimental error being smaller than ±5%.

Computational Details: The calculations were performed using the density functional method B3LYP[37] in conjunction with the 6-311+G(2d,p) basis sets as implemented in the Gaussian03 suite.[38] For all optimized structures, frequency analysis at the same level of theory was used in order to assign them as genuine minima or transition structures as well as to calculate the zero-point vibrational energies (ZPVEs). The transition structures were further characterized by intrinsic reaction-coordinate calculations.[39] The difference between vertical and adiabatic ionization (recombination) energies ($\Delta E_{v/a}$) were calculated as the difference between the energy of an ion (neutral) with optimized geometry and the energy of the same ion (neutral) with the geometry optimized for the corresponding neutral (ion).

Acknowledgments

Financial support by the Deutsche Forschungsgemeinschaft, the Fonds der Chemischen Industrie, and the Gesellschaft von Freunden der Technischen Universität Berlin is gratefully acknowledged.

[1] S. L. Miller, *Science* **1953**, *117*, 528.
[2] E. P. Gardner, J. R. McNesby, *J. Photochem.* **1980**, *13*, 353.
[3] A. Bossard, G. Toupance, *Nature* **1980**, *288*, 243.
[4] Alternatively, methane and ammonia can be coupled also by the assistance of platinum-based catalysts (Degussa process). For a leading reference, see: M. Diefenbach, M. Brönstrup, M. Aschi, D. Schröder, H. Schwarz, *J. Am. Chem. Soc.* **1999**, *121*, 10614.
[5] E. P. Gardner, J. R. McNesby, *J. Phys. Chem.* **1982**, *86*, 2646.
[6] J. V. Michael, W. A. Noyes, *J. Am. Chem. Soc.* **1963**, *85*, 1228.
[7] S. G. Hadley, D. H. Volman, *J. Am. Chem. Soc.* **1967**, *89*, 1053.
[8] G. C. G. Waschewsky, D. C. Kitchen, P. W. Browning, L. J. Butler, *J. Phys. Chem.* **1995**, *99*, 2635.
[9] J. J. Magenheimer, R. E. Varnerin, R. B. Timmons, *J. Phys. Chem.* **1969**, *73*, 3904.
[10] E. Kassab, J. T. Gleghorn, E. M. Evleth, *J. Am. Chem. Soc.* **1983**, *105*, 1746.
[11] K. M. Dunn, K. Morokuma, *J. Phys. Chem.* **1996**, *100*, 123.
[12] H. J. Emeleus, L. J. Jolley, *J. Chem. Soc.* **1935**, 929.
[13] P. W. May, P. R. Burridge, C. A. Rego, R. S. Tsang, M. N. R. Ashfold, K. N. Rosser, R. E. Tanner, D. Cherns, R. Vincent, *Diamond Relat. Mater.* **1996**, *5*, 354.
[14] J. A. Pople, K. Raghavachari, M. J. Frisch, J. S. Binkley, P. v. R. Schleyer, *J. Am. Chem. Soc.* **1983**, *105*, 6389.
[15] R. Q. Zhang, K. L. Han, R. S. Zhu, C. S. Lee, S. T. Lee, *Chem. Phys. Lett.* **2000**, *321*, 101.
[16] F. Tureček, *Top. Curr. Chem.* **2003**, *225*, 77.
[17] C. A. Schalley, G. Hornung, D. Schröder, H. Schwarz, *Chem. Soc. Rev.* **1998**, *27*, 91.
[18] N. Goldberg, H. Schwarz, *Acc. Chem. Res.* **1994**, *27*, 347.
[19] J. L. Holmes, *Mass Spectrom. Rev.* **1989**, *8*, 513.
[20] C. Wesdemiotis, F. W. McLafferty, *Chem. Rev.* **1987**, *87*, 485.
[21] J. K. Terlouw, H. Schwarz, *Angew. Chem.* **1987**, *99*, 829; *Angew. Chem. Int. Ed. Engl.* **1987**, *26*, 805.
[22] C. A. Schalley, G. Hornung, D. Schröder, H. Schwarz, *Int. J. Mass Spectrom. Ion Processes* **1998**, *172*, 181.
[23] V. Q. Nguyen, F. Tureček, *J. Mass Spectrom.* **1996**, *31*, 843.
[24] E. E. Rennie, P. M. Mayer, *J. Chem. Phys.* **2004**, *120*, 10561, and references cited therein.
[25] According to the charge states of the projectile and recovery ions, the various NR experiments are denoted as $^{+}NR^{+}$, $^{+}NR^{-}$, $^{-}NR^{+}$, and $^{-}NR^{-}$, respectively, as suggested by: A. W. McMahon, S. K. Chowdhury, A. G. Harrison, *Org. Mass Spectrom.* **1989**, *24*, 620.
[26] C. Wesdemiotis, R. Feng, P. O. Danis, E. R. Williams, F. W. McLafferty, *J. Am. Chem. Soc.* **1986**, *108*, 5847.
[27] H. Bock, R. Dammel, *J. Am. Chem. Soc.* **1988**, *110*, 5261.
[28] J. Wang, Z. Sun, X. Zhu, X. Yang, M. Ge, D. Wang, *Angew. Chem.* **2001**, *113*, 3145; *Angew. Chem. Int. Ed.* **2001**, *40*, 3055.
[29] H. Schwarz, *Int. J. Mass Spectrom.* **2004**, *237*, 75, and references cited therein.
[30] T. H. Choi, S. T. Park, M. S. Kim, *J. Chem. Phys.* **2001**, *114*, 6051.
[31] A. González-Lafont, M. Moreno, J. M. Lluch, *J. Am. Chem. Soc.* **2004**, *126*, 13089.
[32] S. Villeneuve, P. C. Burgers, *Org. Mass Spectrom.* **1986**, *21*, 733.
[33] D. J. DeFrees, A. D. McLean, *J. Am. Chem. Soc.* **1985**, *107*, 4350.
[34] P. C. Burgers, J. L. Holmes, J. K. Terlouw, *J. Am. Chem. Soc.* **1984**, *106*, 2762.
[35] a) R. Flammang, M. T. Nguyen, G. Bouchoux, P. Gerbaux, *Int. J. Mass Spectrom.* **2000**, *202*, A8–A25; b) P. Gerbaux, C. Wentrup, R. Flammang, *Mass Spectrom. Rev.* **2000**, *19*, 367.
[36] C. A. Schalley, D. Schröder, H. Schwarz, *Int. J. Mass Spectrom. Ion Processes* **1996**, *153*, 173.
[37] a) A. D. Becke, *J. Chem. Phys.* **1993**, *98*, 5648; b) C. Lee, W. Yang, R. G. Parr, *Phys. Rev. B* **1988**, *37*, 785; c) B. Miehlich, A. Savin, H. Stoll, H. Preuss, *Chem. Phys. Lett.* **1989**, *157*, 200; d) S. H. Vosko, L. Wilk, M. Nusair, *Can. J. Phys.* **1980**, *58*, 1200.
[38] M. J. Frisch, G. W. Trucks, H. B. Schlegel, G. E. Scuseria, M. A. Robb, J. R. Cheeseman, J. A. Montgomery, Jr., T. Vreven, K. N. Kudin, J. C. Burant, J. M. Millam, S. S. Iyengar, J. Tomasi, V. Barone, B. Mennucci, M. Cossi, G. Scalmani, N. Rega, G. A. Petersson, H. Nakatsuji, M. Hada, M. Ehara, K. Toyota, R. Fukuda, J. Hasegawa, M. Ishida, T. Nakajima, Y.

Honda, O. Kitao, H. Nakai, M. Klene, X. Li, J. E. Knox, H. P. Hratchian, J. B. Cross, C. Adamo, J. Jaramillo, R. Gomperts, R. E. Stratmann, O. Yazyev, A. J. Austin, R. Cammi, C. Pomelli, J. W. Ochterski, P. Y. Ayala, K. Morokuma, G. A. Voth, P. Salvador, J. J. Dannenberg, V. G. Zakrzewski, S. Dapprich, A. D. Daniels, M. C. Strain, O. Farkas, D. K. Malick, A. D. Rabuck, K. Raghavachari, J. B. Foresman, J. V. Ortiz, Q. Cui, A. G. Baboul, S. Clifford, J. Cioslowski, B. B. Stefanov, G. Liu, A. Liashenko, P. Piskorz, I. Komaromi, R. L. Martin, D. J. Fox, T. Keith, M. A. Al-Laham, C. Y. Peng, A. Nanayakkara, M. Challacombe, P. M. W. Gill, B. Johnson, W. Chen, M. W. Wong, C. Gonzalez, and J. A. Pople, *Gaussian03* (Revision A.1), Gaussian, Inc., Pittsburgh, PA, **2003**.

[39] a) C. Gonzalez, H. B. Schlegel, *J. Chem. Phys.* **1989**, *90*, 2154; b) C. Gonzalez, H. B. Schlegel, *J. Phys. Chem.* **1990**, *94*, 5523.

Received: January 13, 2005

